

RECENT RESULTS FROM CLEO*

KARL BERKELMAN

Cornell University, Ithaca, NY 14853-5001, USA

(Received February 6, 2001)

The CLEO detector at the Cornell Electron-Positron Storage Ring is used for the study of the properties and interactions of the b and c quarks and the τ lepton. I will review recent CLEO data on b physics with special relevance to CP violation: B -meson decays through radiative and gluonic penguin amplitudes and the effects on branching ratios and charge asymmetries of interference between penguin and tree amplitudes in two-body charmless B decays.

PACS numbers: 11.30.Er, 13.25.-k, 13.25.Hw

1. Introduction

The CLEO detector [1] is a typical solenoid-based collider detector with high efficiency and good resolution both for charged particles and for neutrals (π^0 and γ). The data I am reporting were taken up through the year 1999 with two configurations of the detector, called CLEO-II and CLEO-II.V. In both configurations the main tracking element is a 1 meter radius cylindrical drift chamber. This is surrounded by plastic scintillation counters for time of flight measurement and CsI scintillators for shower energy measurement. These are all inside a superconducting magnet coil producing a 1.5 T field. Outside, embedded in the iron flux return are three superlayers of wire chambers for muon detection. In the CLEO-II configuration the innermost tracking element was six layers of straw-tube drift chamber, which was replaced by three layers of double-sided silicon strip detector in CLEO-II.V. Also the argon-ethane gas in the main cylindrical drift chamber was replaced with a helium-propane mixture for better track resolution at low momenta.

About two-thirds of the data are from the upsilon resonance just above B -meson threshold, $e^+e^- \rightarrow \Upsilon(4S) \rightarrow B\bar{B}$; the remainder from just below threshold. Table I lists the integrated luminosity for the four data sets. The

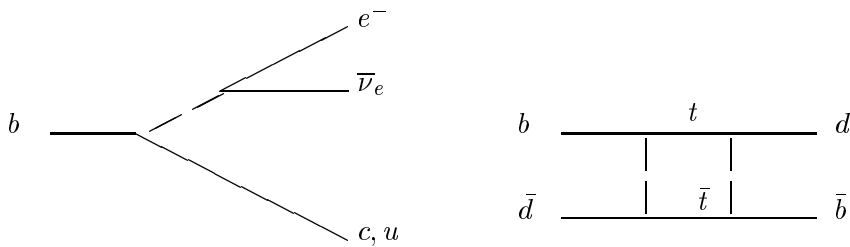
* Presented at the Cracow Epiphany Conference on b Physics and CP Violation, Cracow, Poland, January 5-7, 2001.

data include about 9.7 million $B\bar{B}$ pairs. Since early 2000 CLEO has been running in an upgraded CLEO-III configuration with a similar sized data sample, not yet fully analyzed.

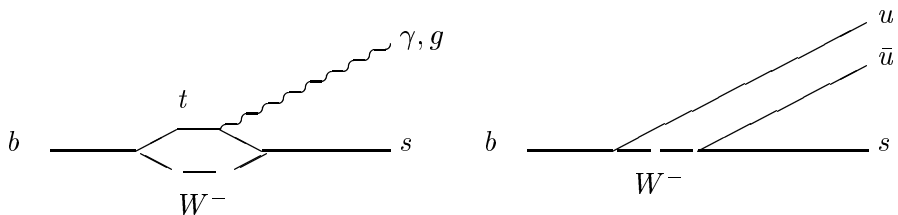
TABLE I

CLEO data sets in fb^{-1} .		
	II	II.V
$\mathcal{T}(4S)$	3.1	6.2
below threshold	1.6	3.0

CLEO b physics in the 1990's has emphasized two areas: (1) the determination of the CKM parameters V_{cb} and V_{ub} from semileptonic decays and V_{td} from $B^0 \leftrightarrow \bar{B}^0$ mixing,



and (2) the study of loop decay processes (so called penguin amplitudes) and their interference with tree decay mechanisms.



Because of time limitations, I will cover only the second area in this talk.

2. Loop dominated decays

2.1. Radiative penguins

The Standard Model forbids first-order $b \rightarrow s$ flavor-changing neutral current transitions. The decay has to proceed through a loop, called a “penguin” diagram, involving the W and an up-type quark u , c , or t . The first radiative penguin process to be studied was the exclusive decay $B \rightarrow K^* \gamma$ [2]. The mode is experimentally rather straightforward to reconstruct with no serious background. Table II lists the updated branching ratios from CLEO.

TABLE II

$B \rightarrow K^* \gamma$ branching ratios in units of 10^{-5} .

	$Br..10^{-5}$
$B^0 \rightarrow K^{*0} \gamma$	$4.55_{-0.68}^{+0.72} \pm 0.34$
$B^+ \rightarrow K^{*+} \gamma$	$3.76_{-0.83}^{+0.89} \pm 0.28$
$B \rightarrow K_2(1430) \gamma$	$1.66_{-0.53}^{+0.59} \pm 0.13$

Although the exclusive measurement is clean, the interpretation in terms of the $b \rightarrow s \gamma$ quark-level process is cloud ed by hadronic uncertainties. More interesting is the inclusive measurement of $B \rightarrow X_s \gamma$. It has no unique experimental signature, however, and is vulnerable to large photon backgrounds from initial state radiation and from π and η decays. To suppress the background CLEO uses a neural net parameter that combines several event topology variables and the χ^2 for the best $X_s = K^{\pm,0} + n\pi$ hypothesis. Since much of the background comes from non- $B\bar{B}$ events, we subtract the rate measured in the data from below $B\bar{B}$ threshold. The updated result [3] is:

$$Br(B \rightarrow X_s \gamma) = (3.15 \pm 0.35 \pm 0.32 \pm 0.26) \times 10^{-4} \quad (\text{CLEO}).$$

There are more data in the pipeline, and I expect that the accuracy will improve soon. The measured rate is consistent with the next-to-leading order Standard Model calculation [4],

$$Br(B \rightarrow X_s \gamma) = (3.71 \pm 0.38) \times 10^{-4} \quad (\text{theory}).$$

The agreement places strong constraints on physics beyond the Standard Model contributing in the loop: charged Higgs, non-standard couplings, *etc.* [5].

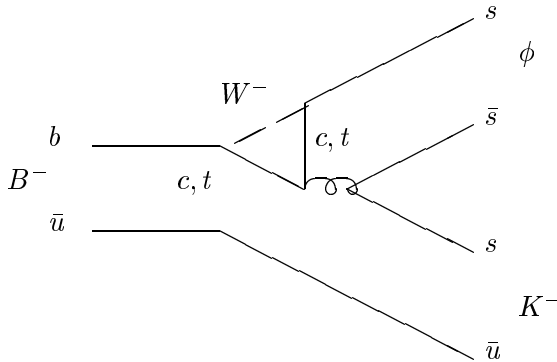
With the subset of the $B \rightarrow X_s \gamma$ data sample in which there is a favored $X_s^\pm = K^\pm + n\pi$ hypothesis or a lepton tag from the other B we can measure the charge asymmetry and look for direct CP violation in the decay. This has very recently been done by CLEO with the result [6]

$$\mathcal{A}_{CP} = \frac{b - \bar{b}}{b + \bar{b}} = (-0.079 \pm 0.108 \pm 0.022) \times (1 \pm 0.03).$$

The asymmetry is consistent with zero, as one would expect in the case of a single dominant amplitude. This result restricts possible new physics mechanisms in the loop interfering with the Standard Model amplitude [5].

2.2. Gluonic penguins

The gluonic $b \rightarrow sg$ loop process usually results in a hadronic final state that can be reached also through a simple tree diagram. To be sure that we have seen a gluonic penguin we have to look for a final state containing quarks that cannot be produced except through $b \rightarrow sg$, for example, $B \rightarrow \phi K$.



In principle, the annihilation diagram ($b \bar{u} \rightarrow W \rightarrow \dots$) and the penguin annihilation diagram ($b \bar{d} \rightarrow g \rightarrow \dots$) are also possible, but their contributions are expected to be highly CKM suppressed. CLEO has now seen these decays and also the modes with K^* (see Table III), using a likelihood analysis employing distributions in M_B , ΔE , m_ϕ , $\cos \theta_{tt}$, and $\cos \theta_{\text{hel}}$. The rates confirm expectations for gluonic penguin dominance [7], suppressed by the loop, by the $g \rightarrow s\bar{s}$ fraction, and by the exclusive/inclusive fraction.

TABLE III

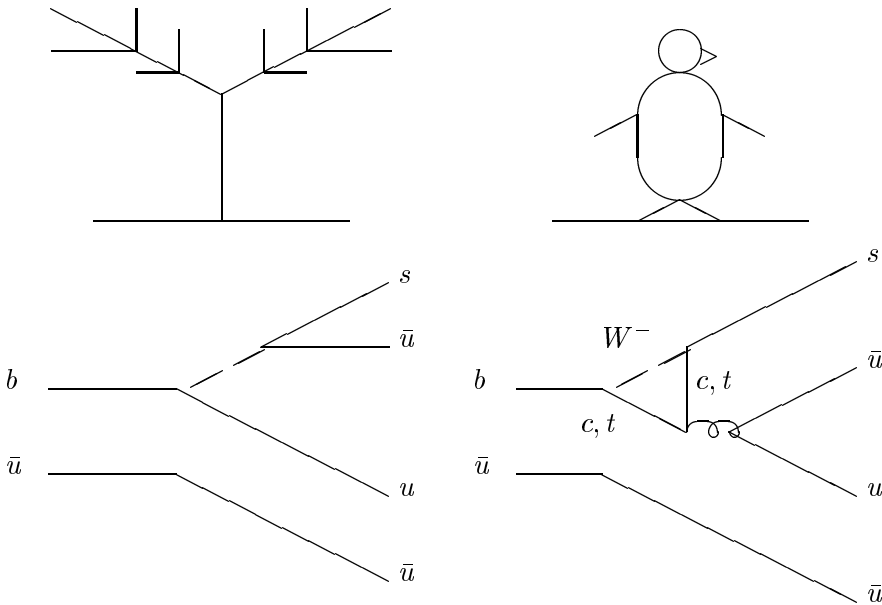
CLEO $B \rightarrow \phi K^{(*)}$ branching ratios in units of 10^{-6} .

	$B \rightarrow \phi K$	$B \rightarrow \phi K^*$
$+ \rightarrow +$	$5.5^{+2.1}_{-1.8} \pm 0.6$	$10.6^{+6.4+1.2+2.3}_{-4.9-1.6-0.7}$
$0 \rightarrow 0$	$5.4^{+3.7}_{-2.7} \pm 0.7$	$11.5^{+4.5+1.3+2.1}_{-3.7-1.5-1.6}$
average	$5.5^{+1.8}_{-1.5} \pm 0.7$	$11.2^{+3.6+1.3+2.1}_{-3.1-1.5-1.3}$

3. Tree and loop interference

3.1. Contributing amplitudes

We expect that many hadronic B decays to two-body final states not containing charm proceed through two interfering amplitudes, a $b \rightarrow uW$ tree diagram and a $b \rightarrow sg$ penguin loop. An example is $B^- \rightarrow K^- \pi^0$.



In terms of the Wolfenstein parametrization [8] of the CKM matrix [9], the amplitudes contain:

$$\text{Tree} \propto V_{ub}V_{us}^* \sim A\lambda^4 \sqrt{\rho^2 + \eta^2} e^{i\gamma},$$

$$\text{Penguin} \propto V_{Qb}V_{Qs}^* \sim A\lambda^2 e^{i\phi} \quad (Q = c, t),$$

where the weak phase γ is $\arg(\rho + i\eta)$, and the strong phase ϕ comes mainly from final state re-scattering and the fact that the $c\bar{c}$ in the loop can be on the mass shell. There are typically also contributions from electroweak penguins (replacing the gluon with γ or Z) and from final state interactions.

3.2. CLEO measurements

Measurements of the branching ratios are not simple. Since the signals are small ($\mathcal{B}r \lesssim 10^{-5}$), one has to fix one's strategy for extracting them before looking at the data to avoid chasing after background fluctuations. The backgrounds are large and easily confused. For the $B \rightarrow PP$ modes they come mainly from 2-jet $e^+e^- \rightarrow u\bar{u}$, $d\bar{d}$, or $s\bar{s}$. The $B \rightarrow PV$ modes are also vulnerable to $e^+e^- \rightarrow c\bar{c}$ and $b\bar{b}$ backgrounds. We use the beam-constrained reconstructed mass M_B , the energy conservation ΔE , and several measures of jettiness to characterize the candidates. These may be combined into one Fisher or neural net variable. Then we do either a traditional cut procedure or a maximum likelihood analysis, using Monte Carlo signal and background samples to optimize the cuts and/or determine the probability density functions. The non- $B\bar{B}$ background is subtracted using below threshold data.

Although it is not a problem in the current CLEO-III configuration, distinguishing charged kaons and pions at high momenta was difficult in the CLEO-II and II.V configurations. We use dE/dx and the energy balance kinematics. The distributions for kaons and pions overlap in each of the two variables. In CLEO-II we get 1.7σ separation from each, and in CLEO-II.V we get 2σ from each. This allows us, for example, to make a statistical separation of $K^+\pi^-$ and $\pi^+\pi^-$ provided that the rates are not too different. The significance of the sum signal and the separation significance can be gauged with likelihood contours in the $N(\pi\pi)$ versus $N(K\pi)$ plane (see Ref. [10] for instance).

The latest CLEO branching ratio measurements [10–13] are listed in Tables IV, V, and VI. In some modes there are compatible results also from the BaBar and BELLE experiments [14,15].

TABLE IV

CLEO branching ratios and 90% confidence upper limits for charmless PP modes, in units of 10^{-6} .

$B \rightarrow PP$	$Br..10^{-6}$	$B \rightarrow PP$	$Br..10^{-6}$
$K^+ \pi^-$	$17.2^{+2.5}_{-2.4} \pm 1.2$	$\pi^+ \pi^-$	$4.3^{+1.6}_{-1.4} \pm 0.5$
$K^- \pi^0$	$11.6^{+3.0+1.4}_{-2.7-1.3}$	$\pi^- \pi^0$	< 12.7
$\bar{K}^0 \pi^-$	$18.2^{+4.6}_{-4.0} \pm 1.6$		
$\bar{K}^0 \pi^0$	$14.6^{+5.9+2.4}_{-5.1-3.3}$	$\pi^0 \pi^0$	< 5.7
$K^- \eta$	< 6.9	$\pi^- \eta$	< 5.7
$\bar{K}^0 \eta$	< 9.3	$\pi^0 \eta$	< 2.9
$K^- \eta'$	$80^{+10}_{-9} \pm 7$	$\pi^- \eta'$	< 12
$\bar{K}^0 \eta'$	$89^{+18}_{-16} \pm 9$	$\pi^0 \eta'$	< 5.7
$K^+ K^-$	< 1.9	$K^- K^0$	< 5.1

TABLE V

CLEO branching ratios and 90% confidence upper limits for charmless PV modes, in units of 10^{-6} .

$B \rightarrow PV$	$Br..10^{-6}$	$B \rightarrow PV$	$Br..10^{-6}$
$K^- \rho^+$	< 32	$\pi^- \rho^+$	$27.6^{+8.4}_{-7.4} \pm 4.2$
$K^- \rho^0$	< 17	$\pi^- \rho^0$	$10.4^{+3.3}_{-3.4} \pm 2.1$
		$\pi^0 \rho^-$	< 43
$\bar{K}^0 \rho^0$	< 27	$\pi^0 \rho^0$	< 5.5
$K^- \omega$	< 7.9	$\pi^- \omega$	$11.3^{+3.3}_{-2.9} \pm 1.4$
$\bar{K}^0 \omega$	< 21	$\pi^0 \omega$	< 5.5
$K^- \phi$	$5.5^{+2.1}_{-1.8} \pm 0.6$	$\pi^- \phi$	< 4.0
$\bar{K}^0 \phi$	$5.4^{+3.7}_{-2.7} \pm 0.7$	$\pi^0 \phi$	< 5.4
ηK^{*-}	$26.4^{+9.6}_{-8.2} \pm 3.0$	$\eta \rho^-$	< 15
$\eta \bar{K}^{*0}$	$13.8^{+5.5}_{-4.6} \pm 1.6$	$\eta \rho^0$	< 10
$\eta' K^{*-}$	< 35	$\eta' \rho^-$	< 33
$\eta' \bar{K}^{*0}$	< 21	$\eta' \rho^0$	< 12
$K^- K^{*+}$	< 6	$\pi^+ K^{*-}$	22^{+8+4}_{-6-5}
$K^- K^{*0}$	< 5.3	$\pi^- \bar{K}^{*0}$	< 16
$\pi^0 K^{*0}$	< 3.6	$\pi^0 K^{*-}$	< 31

TABLE VI

CLEO branching ratios and 90% confidence upper limits for charmless VV modes, in units of 10^{-6} .

$B \rightarrow VV$	$Br..10^{-6}$	$B \rightarrow VV$	$Br..10^{-6}$
$\rho^0 \rho^0$	< 5.9		
$\rho^0 K^{*-}$	< 9.5	$\bar{K}^{*0} K^{*+}$	< 50
$\rho^0 \bar{K}^{*0}$	< 19	$\bar{K}^{*0} K^{*0}$	< 10
ϕK^{*-}	$10.6^{+6.4+1.2+2.3}_{-4.9-1.6-0.7}$	$K^{*-} K^{*+}$	< 70
$\phi \bar{K}^{*0}$	$11.5^{+4.5+1.3+2.1}_{-3.7-1.5-1.6}$	$\bar{K}^{*0} \bar{K}^{*0}$	< 31

3.3. Interpretation

There are several qualitative observations that one can draw from these measurements.

- The branching fractions for the $K\pi$ modes are more than three times as large as for the $\pi\pi$ modes. Since the tree diagram is suppressed by λ^4 in $K\pi$ and only by λ^3 in $\pi\pi$, this indicates that at least the $\bar{K}\pi$ amplitudes must be dominantly penguin. The $\pi\pi$ is likely also to have a non-negligible penguin contribution. The small branching ratio and the penguin “pollution” combine to make $\pi^+\pi^-$ less attractive for indirect CP violation studies than originally thought.
- The $\rho\pi$ branching fractions are larger than the $\pi\pi$. Although $\rho^+\pi^-$ is not a CP eigenstate, it may be a useful substitute for $\pi^+\pi^-$ in indirect CP violation measurements.
- The $\eta'K$ mode is by far the most copious of the two-body charmless B decay modes. In contrast, the as yet undetected ηK branching ratio is more than an order of magnitude smaller. No one anticipated this. A satisfactory explanation may involve Zweig violating $b \rightarrow sgg$, $gg \rightarrow \eta'$ or $c\bar{c}$ admixture in the η' state (with $b \rightarrow cW$, $W \rightarrow \bar{c}s$). The measured ηK^* branching ratio may provide a clue.

To be more quantitative, we note that the branching ratio for a tree+loop decay contains an interference term proportional to $\cos\gamma \cos\phi$, where γ is the weak phase corresponding to $\rho + i\eta$ and ϕ is the strong phase difference, varying with decay channel and depending on non-perturbative final state interaction physics. One has to combine data from several modes, using isospin and SU(3) relations, to untangle the dependences on ϕ and extract a value for γ . Triangle and quadrangle relations [16], inequalities [17],

and model dependent global fits [18] have been suggested in the literature. Fitting with a naive factorization model [19] suggests $\gamma > 90^\circ$, which contradicts constraints from $B^0 - \bar{B}^0$ and $B_s^0 - \bar{B}_s^0$ mixing data. If this were to hold up, it would be an indication that the weak phase does not come entirely from the CKM matrix. However, fits of the branching ratio data with more sophisticated versions of the factorization model [18] can be made consistent with $\gamma < 90^\circ$.

4. CP violation

4.1. CKM framework

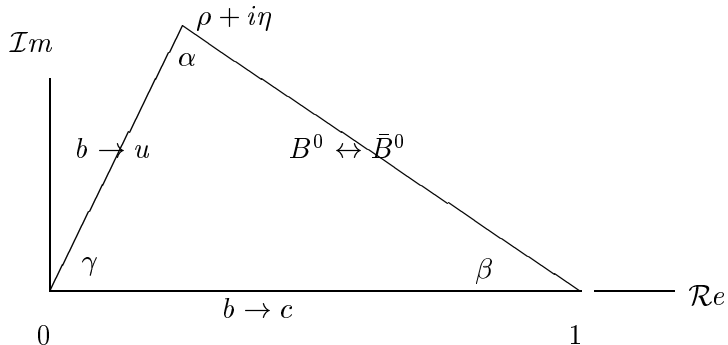
I am the first speaker at the conference to mention CP violation in B decays, so I should summarize briefly the Standard Model framework. Since the weak interaction eigenstates are not flavor eigenstates, the amplitudes for the flavor changing weak quark transitions involve the elements of the unitary Cabibbo–Kobayashi–Maskawa matrix [9] that connects weak and flavor eigenstates:

$$\begin{vmatrix} V_{ud} & V_{us} & V_{ub} \\ V_{cd} & V_{cs} & V_{cb} \\ V_{td} & V_{ts} & V_{tb} \end{vmatrix}.$$

There are only four independent parameters, which allows us to rewrite the matrix in the Wolfenstein scheme [8]

$$\begin{vmatrix} 1 - \lambda^2/2 & \lambda & A\lambda^3(\rho - i\eta) \\ -\lambda & 1 - \lambda^2/2 & A\lambda^2 \\ A\lambda^3(1 - \rho - i\eta) & -A\lambda^2 & 1 \end{vmatrix}.$$

We know the Cabibbo angle $\lambda \approx 0.22$ and $A \approx 0.8$. Our ignorance of the remaining ρ and η parameters is best expressed as the apex of the Unitarity Triangle, representing $V_{td}V_{tb}^* + V_{cd}V_{cb}^* + V_{ud}V_{ub}^* = 0$ and plotted in the complex plane with the base ($V_{cd}V_{cb}^*$) normalized to one.



The lengths of the sides of the triangle relate to the b decay and mixing measurements noted on the figure.

An important goal of future b physics experiments is to refine the measurements of the sides of the triangle and independently measure the angles α , β , and γ by measuring the phases of the $b \rightarrow c$ and $b \rightarrow u$ amplitudes and the phase of $B - \bar{B}$ mixing. This will complete the measurement of the basic parameters of the Standard Model, test its validity, and perhaps reveal physics beyond. We will also be able to tell whether CP violation comes only through the nonzero imaginary term $i\eta$ in the CKM matrix or whether there is another source of CP violation beyond the Standard Model.

4.2. Direct CP asymmetries

As I have discussed above, tree + loop amplitudes can produce an interference term in CP -averaged branching ratios proportional to $\cos\gamma \cos\phi$. The interference can also produce a decay rate CP asymmetry (called “direct” CP violation) proportional to $\sin\gamma \sin\phi$. Note that depending on whether the strong phase difference ϕ turns out to be large or small, there will be sensitivity to the weak phase γ either in the averaged branching ratios or in the asymmetries.

Provided there are enough data and the backgrounds can be handled, the measurement of \mathcal{A}_{CP} is a straightforward counting of charge conjugate modes: $K^+\pi^-$ versus $K^-\pi^+$, for instance, or substituting K^* for K , and/or π^0 , η , η' , ρ , ω for π^\pm . There is no need to tag the other B , and since the time evolution is not required, there is no advantage in boosting the $B\bar{B}$ frame by colliding unequal beam energies. This makes the study of direct CP violation a natural goal for the CLEO experiment at CESR. For five of the charmless two-body B decay modes there are enough events

TABLE VII

CLEO direct CP asymmetry measurements.

	\mathcal{A}_{CP}
$K^-\pi^+$	-0.04 ± 0.16
$K^-\pi^0$	-0.29 ± 0.23
$K_S\pi^-$	$+0.18 \pm 0.24$
$K^-\eta'$	$+0.03 \pm 0.12$
$\pi^-\omega$	-0.34 ± 0.25
ψK^-	$+0.018 \pm 0.043 \pm 0.004$
$\psi' K^-$	$+0.020 \pm 0.091 \pm 0.010$
$X_s\gamma$	$-0.079 \pm 0.108 \pm 0.022$

to allow a measurement of $\mathcal{A}_{CP} = (\bar{B} - B)/(\bar{B} + B)$. The results [20] are in Table VII, along with asymmetries from two $\psi^{(l)}K$ modes [21] and the already mentioned $B \rightarrow X_s \gamma$ result.

The charmless two-body B decay asymmetries are so far all consistent with zero. One can probably conclude that the strong phases ϕ are not large. There is still the problem of un-tangling the dependences on the strong phase in order to extract information on the weak phases. For that we will need more accurate data and more modes.

4.3. Indirect CP asymmetries

Another process that is sensitive to weak phases is the CP asymmetry that comes from the interference between a single decay amplitude and $B - \bar{B}$ mixing, called “indirect” CP violation. To measure the asymmetry one has to tag the flavor (B versus \bar{B}) of the other B and observe the time evolution of the decay, which requires a boosted $B\bar{B}$ frame and unequal colliding beam energies. Indirect CP violation is therefore not easily observed at CESR. However, there are a number of CLEO measurements at CESR that are relevant to the study of indirect CP asymmetries.

The Standard Model predicts zero for the phase of $b \rightarrow c$, γ for the phase of $b \rightarrow u$, and β for the phase of mixing. The interference between unmixed $B^0 \rightarrow \psi K_S^0$ and mixed $B^0 \rightarrow \bar{B}^0 \rightarrow \psi K_S^0$ should therefore produce $\mathcal{A}_{CP} \propto \sin 2\beta$, provided that only $b \rightarrow c$ is involved in the decay to ψK . The CLEO measurement consistent with zero direct CP asymmetry in $B^\pm \rightarrow \psi K^\pm$ decay supports the assumption of a single $b \rightarrow c$ decay amplitude. The corresponding hypothesis for $B \rightarrow \pi^+ \pi^-$, that it is a pure $b \rightarrow u$ decay, is probably not valid, given the conclusion from the CLEO $K\pi$ and $\pi\pi$ branching ratio data that there is sizeable penguin contribution competing with $b \rightarrow u$.

CLEO has now compiled a good number of branching ratio measurements for charmonium modes related to ψK_S^0 [22], some of which may be useful for indirect CP violation measurements of $\sin 2\beta$ — $\psi' K_S^0$ and $\chi_{c1} K_S^0$ for instance. These are listed in Table VIII. However, CLEO’s angular analysis of $B \rightarrow \psi^{(l)} K^{*0} (\rightarrow K_S^0 \pi^0)$ indicates both S and P wave contributions, making it less suitable for measurement of $\sin 2\beta$.

I summarize in Table IX the experimental data on $\sin 2\beta$ as of the time of the summer 2000 Osaka conference, from early measurements on $B \rightarrow \psi K_S^0$ at LEP [23], the Tevatron [24], and the asymmetric e^+e^- colliders [14], [15]. From the comparison of the average with the value derived from data on the sides of the unitarity triangle [25] (much of it from CLEO) there is no evidence yet of a deviation from Standard Model expectations. Note that the uncertainty in the $\sin 2\beta$ derived from the unitarity triangle sides is dominantly theoretical. Various analyses assign different error limits.

TABLE VIII

CLEO branching ratios and 90% confidence upper limits for $B \rightarrow (c\bar{c})K^{(*)}$, in units of 10^{-4} .

$Br..10^{-4}$		$Br..10^{-4}$	
ψK^+	$10.2 \pm 0.8 \pm 0.7$	ψK^0	$9.5 \pm 0.8 \pm 0.6$
$\psi' K^+$	$7.8 \pm 0.7 \pm 0.9$	$\psi' K^0$	$5.0 \pm 1.1 \pm 0.5$
ψK^{*+}	$14.1 \pm 2.3 \pm 2.4$	ψK^{*0}	$13.2 \pm 1.7 \pm 1.7$
$\psi' K^{*+}$	$9.2 \pm 1.9 \pm 1.2$	$\psi' K^{*0}$	$7.6 \pm 1.1 \pm 1.0$
$\eta_c K^+$	$6.9_{-2.1}^{+2.6} \pm 0.8 \pm 2.0$	$\eta_c K^0$	$10.9_{-4.2}^{+5.5} \pm 1.2 \pm 3.1$
$\chi_{c0} K^+$	< 4.8	$\chi_{c0} K^0$	< 5.0
$\chi_{c1} K^+$	$8.7 \pm 2.5 \pm 0.9$	$\chi_{c1} K^0$	$3.9_{-1.3}^{+1.9} \pm 0.4$

TABLE IX

Measurements of $\sin 2\beta$ as of summer 2000.

$\sin 2\beta$	
OPAL [23]	$3.2_{-2.0}^{+1.8} \pm 0.5$
ALEPH [23]	$0.93_{-0.88-0.24}^{+0.64+0.36}$
CDF [24]	$0.79_{-0.44}^{+0.41}$
BaBar [14]	$0.12 \pm 0.36 \pm 0.9$
BELLE [15]	$0.45_{-0.44-0.09}^{+0.43+0.07}$
Average ψK	0.49 ± 0.23
Triangle sides	0.72 ± 0.1

5. Conclusions

There is now an extensive data base for understanding hadronic B decays: branching ratios and upper limits down to the level of a few times 10^{-6} , angular distributions for vector modes, direct CP asymmetries at the level of ± 0.1 to 0.2 for several charmless modes, and indirect CP asymmetries for $B \rightarrow \psi K_S^0$ with a combined accuracy around ± 0.2 . At the rate they are now taking data the e^+e^- colliders operating at the $\Upsilon(4S)$ can expand this data base rapidly, and we can anticipate exciting new insights in the next few years.

So far the data confirm the Standard Model. In particular, CLEO B decay data confirm the expectations for flavor changing neutral currents through the penguin loop amplitude. Essentially pure penguin processes have been measured for $b \rightarrow s\gamma$ and $b \rightarrow s$ *gluon*, and the results restrict the range of new physics allowable. The direct CP asymmetry is consistent with zero for the modes that one expects to be free of interference: $B \rightarrow \psi K$ and $B \rightarrow X_s\gamma$. Factorization models of two-body hadronic decays have to become more sophisticated than the naive early versions in order to be compatible with the data.

So far the various measurements that relate to the Unitarity Triangle appear to be consistent: $b \rightarrow cl\nu$, $b \rightarrow ul\nu$, $B^0 \leftrightarrow \bar{B}^0$, $B_s^0 \leftrightarrow \bar{B}_s^0$, ϵ_K , γ (from $B \rightarrow K\pi, \dots$), and $\sin 2\beta$ from mixing-mediated indirect CP violation in ψK_S^0 . CP violation in B decay has been seen at the level of two standard deviations.

6. Postscript: the future of CESR and CLEO

The CLEO collaboration has recently completed and installed an upgrade of the detector, now called CLEO-III. The new components are:

- a four-layer double-sided silicon-strip detector for precision tracking near the beam line,
- a ring-imaging Cherenkov detector for charged $\pi/K/p$ separation at high momentum,
- a cylindrical drift chamber, reconfigured to leave space for the Cherenkov system and for closer beam focusing,
- faster data readout electronics.

The new detector has been taking data since spring 2000.

The upgrade of the CESR collider has been proceeding in stages. The upgrade includes:

- superconducting rf cavities for high stable beam currents,
- improvements in positron production and in linac and synchrotron injection intensities,
- upgraded vacuum hardware to handle higher beam currents,
- superconducting final focus quadrupole magnets for lower β^* at the interaction point.

All of this is operating now except the superconducting quads, which are fabricated and tested but not yet installed. The peak luminosity has tripled since before the first of the four superconducting rf cavities was installed; it is now at the level of $1.2 \times 10^{33} \text{ cm}^{-2}\text{s}^{-1}$.

Until recently, CESR led all colliders in luminosity. There is now strong competition though from PEP-2 and KEK-B, which have the advantage of being able to circulate electron and positron beams in separate vacuum chambers. The luminosity record is now held by PEP-2 at around $3 \times 10^{33} \text{ cm}^{-2}\text{s}^{-1}$. For indirect CP violation measurements PEP-2 and KEK-B also have the advantage of unequal beam energies. Provided the completion of the CESR luminosity upgrade (the superconducting final focus quads) is successful in giving CESR a competitive luminosity, there are still plenty of good B physics opportunities for a symmetric-energy collider:

- improved V_{cb} , V_{ub} , V_{td} , and V_{ts} measurements,
- rare B decays and tests of the Standard Model,
- direct CP violation.

CESR and CLEO will likely continue B physics at the $\Upsilon(4S)$, at least for several years.

Meanwhile at Cornell we are examining the possibility of modifying CESR to run at high luminosity ($\mathcal{L}_{pk} > 10^{32}$) at low energy, near $c\bar{c}$ threshold. This would allow CLEO to pursue precision D and D_s physics:

- V_{cd} and V_{cs} ,
- $D^0\bar{D}^0$ mixing and CP violation,
- $D_{(s)} \rightarrow \mu\nu$ and $f_{D(s)}$,
- rare D decays and tests of the Standard Model and Heavy Quark Effective Theory.

CESR would also be useful for precision τ lepton physics:

- measurement of the mass of the τ_ν ,
- rare decays and tests of the Standard Model.

The accelerator group is continuing its basic research work on superconducting rf cavities for use in future machines, such as

- a TeV linear e^+e^- collider (TESLA, say),
- a muon storage ring for neutrino physics,
- a $\mu^+\mu^-$ collider.

REFERENCES

- [1] Y. Kubota *et al.*, (CLEO), *Nucl. Instrum. Methods Phys. Res.* **A320**, 66 (1992); T. Hill *et al.*, (CLEO), *Nucl. Instrum. Methods Phys. Res.* **A418**, 32 (1998).
- [2] T.E. Coan *et al.*, (CLEO), *Phys. Rev. Lett.* **84**, 5283 (2000); R. Ammar *et al.*, (CLEO), *Phys. Rev. Lett.* **71**, 674 (1993).
- [3] M.S. Alam *et al.*, (CLEO), *Phys. Rev. Lett.* **74**, 2885 (1995).
- [4] M. Misiak, *Acta Phys. Pol.* **B32**, 1879 (2001).
- [5] A.L. Kagan, M. Neubert, *Phys. Rev.* **D58**, 09412 (1998); M. Aoki, G. Cho, N. Oshimo, *Phys. Rev.* **D60**, 035004 (1999).
- [6] T.E. Coan *et al.*, (CLEO), CLNS 00/1697.
- [7] N.G. Deshpande, Xiao-Gang He, *Phys. Lett.* **B336**, 471 (1994).
- [8] L. Wolfenstein, *Phys. Rev.* **D31**, 2381 (1985).
- [9] M. Kobayashi, T. Maskawa, *Prog. Theor. Phys.* **49**, 652 (1973).
- [10] D. Cronin-Hennessy *et al.*, (CLEO), *Phys. Rev. Lett.* **85**, 515 (2000).
- [11] S.J. Richichi *et al.*, (CLEO), *Phys. Rev. Lett.* **85**, 520 (2000).
- [12] C.P. Jessop *et al.*, (CLEO), CLNS 99/1652.
- [13] R. Godang *et al.*, (CLEO), CLNS 00/1705, hep-ex/0101029.
- [14] V. Shelkov, *Acta Phys. Pol.* **B32**, 000 (2001); BaBar Collaboration, reported at the XXXth International Conference on High Energy Physics, Osaka, Japan, July 2000.
- [15] K. Miyabayashi, *Acta Phys. Pol.* **B32**, 1663 (2001); BELLE Collaboration, reported at the XXXth International Conference on High Energy Physics, Osaka, Japan, July 2000.
- [16] See for instance M. Gronau, J.L. Rosner, D. London, *Phys. Rev. Lett.* **73**, 21 (1994).
- [17] See for instance R. Fleischer, T. Mannel, *Phys. Rev.* **D57**, 2752 (1998).
- [18] C. Sachrajda, *Acta Phys. Pol.* **B32**, 1821 (2001).
- [19] See for instance W.-S. Hou, J.G. Smith, F. Wurthwein, hep-ex-9910013.
- [20] S. Chen *et al.*, (CLEO), CLNS 99/1651.
- [21] G. Bonvicini *et al.*, (CLEO), *Phys. Rev. Lett.* **84**, 5940 (2000).
- [22] K.W. Edwards *et al.*, (CLEO), hep-ex/0007012; G. Brandenburg *et al.*, (CLEO), hep-ex/0007046; P. Avery *et al.*, (CLEO), *Phys. Rev.* **D84**, 5940 (2000).
- [23] T. Lesiak, *Acta Phys. Pol.* **B32**, 1711 (2001); OPAL collaboration, *Eur. Phys. J.* **C5**, 370 (1998); ALEPH collaboration, CERN-EP/2000-105.
- [24] S. Tkaczyk, *Acta Phys. Pol.* **B32**, 1747 (2001).
- [25] A. Ali, *Acta Phys. Pol.* **B32**, to be published.